A Compression Scheme for Enhanced Demura Performance in AMOLED Displays

Chunhui Ren*, Fei Fang*,Hao Ji*, Xiaoping Tan*, Mingwei Ge*, Ying Shen *

***Kunshan Govisionox Optoelectronics Co., Ltd, China**

Abstract

Against the backdrop of ongoing advancements in display technology, the storage efficiency of Demura compensation data for display panels has emerged as a pivotal factor constraining both performance enhancement and cost management in high-end display devices. To tackle this challenge, this study innovatively introduces an efficient compression scheme that synergizes multi-dimensional feature extraction optimization with adaptive encoding strategies. Through multi-scale separation of image compensation data and leveraging structural similarity among segmented images, the scheme achieves shared image structures for multi-brightness compensation data, elevating the compression ratio to over 9 times while significantly reducing decompression computational complexity. Real-world testing on AMOLED panels confirms that the decompressed images attain an average Peak Signal-to-Noise Ratio (PSNR) of 41.4 dB and a Structural Similarity Index (SSIM) of 0.950, cutting storage space requirements by 50% compared to existing techniques, with a mere 50-80K gate count for the decompression IP circuit chip. This approach offers an effective solution for SRAM storage optimization in high-end displays and high-resolution scenarios.

Author Keywords

Image Compression; Demura; SRAM; PSNR;SSIM;

1. Background

AMOLED (Active Matrix Organic Light-Emitting Diode) technology has become the mainstream solution for high-end display devices, thanks to its advantages such as high contrast, ultra-thin design, and flexibility. However, constrained by the uniformity of thin-film transistor (TFT) processes, TFTs at different positions on large-area substrates exhibit variations in parameters like threshold voltage and mobility. This leads to Mura phenomena, such as uneven brightness or color deviation in displayed images, directly impacting yield rates and user experience.

To address this issue, external optical compensation (Demura) technology has emerged [1]. This technology employs high-precision CCD cameras to capture display image data, identify Mura regions, and generate compensation data, which is then written into the driver IC for real-time correction. During this process, data compression technology plays a critical role: on one hand, the vast volume of compensation data for high-resolution AMOLED screens necessitates compression to reduce storage space and transmission bandwidth; on the other hand, the compression algorithm must balance decompression efficiency and accuracy to avoid introducing distortions after decompression. Therefore, compression algorithms with high compression ratios and low hardware complexity have become a core competitive advantage of Demura technology [2].

2. Methods

2.1 Multi-Scale Separation of Mura Defects

In AMOLED display technology, the Mura phenomenon represents a critical issue affecting image quality and can be categorized into three types: DC Mura, AC Mura, and Sandy Mura, each with distinct causes and manifestations.

DC Mura manifests as fixed-position brightness or color deviation anomalies in the display, originating from static defects in the manufacturing process. During thin-film deposition, uneven gas flow and electric field distributions within the chamber of PECVD (Plasma-Enhanced Chemical Vapor Deposition) or PVD (Physical Vapor Deposition) equipment lead to in-plane variations in insulating or metallic film thickness. These variations subsequently alter TFT electrical parameters, causing localized current irregularities and resulting in position-fixed Mura defects. Similarly, non-uniform electric and fluid fields during etching processes may induce local depth variations, contributing to uneven brightness. Such defects persist in static images.

AC Mura is characterized by periodic brightness or color deviations that vary over time, often linked to drive system instability [3]. Fluctuations in driver IC output signals or unstable power supply voltages can induce dynamic pixel brightness shifts. For instance, during dynamic video playback, periodic driver signal jitter may cause specific screen regions to alternately brighten or dim, resembling a "breathing" effect. This dynamic Mura severely degrades viewing experience.

Sandy Mura, named for its grain-like appearance, arises from cumulative pixel-level microdefects. These may stem from subtle inhomogeneities during OLED material deposition or parameter deviations in individual TFTs within the array, leading to fine, scattered brightness variations. From a distance, the screen appears speckled with sand-like particles, while close inspection reveals irregular, densely packed spots, significantly reducing display smoothness and uniformity.

In this study, DC Mura, AC Mura, and Sandy Mura were separated from Mura data using multi-scale separation techniques. As shown in Figure 1, Sandy Mura accounts for over 90% of the total data volume in terms of spatial occupancy.

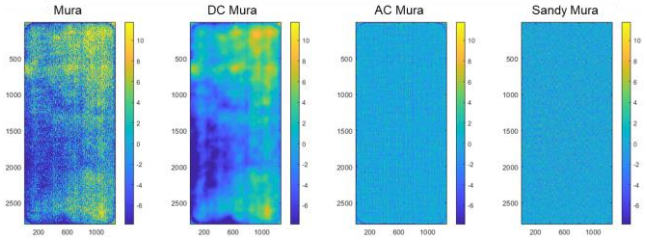

Figure 1. Characteristics of DC, AC, and Sandy Mura Defects.

2.2 Mura data Characteristics Under Varying Brightness Levels

In AMOLED display technology, the Mura phenomenon—a critical factor affecting image quality—can be categorized into three primary types: DC Mura, AC Mura, and Sandy Mura. Their manifestation characteristics are influenced not only by manufacturing processes but also by driving technologies such as dimming architectures, dynamic Vref voltage adjustments, and dynamic ELVSS (Electrode Line Voltage for Source Side) voltage modulation. These factors induce dynamic variations in Mura behavior across different brightness levels.

As illustrated in Figure 2, while the core characteristics of Mura defects remain similar across brightness conditions, localized changes may occur, including:

1. Emergence of new Mura types in specific brightness ranges.
2. Alterations in intensity (e.g., enhanced or diminished contrast) of existing Mura.
3. Shifts in spatial distribution (e.g., expanded or contracted affected areas).

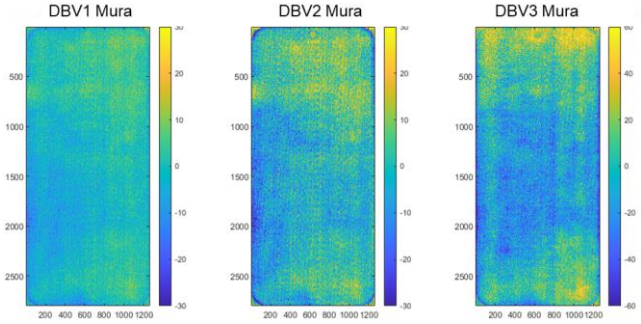

Figure 2. Comparative Analysis of Mura Defects Across Brightness Levels.

2.3 Multi-Scale Separation of Image Compensation data

As illustrated in Figure 3, this study employs multi-scale separation techniques to process Demura data, accurately dividing it into three components: DC data, AC data, and Sandy data [4]. This separation strategy creates favorable conditions for subsequent data compression, enabling more targeted processing and significantly enhancing both efficiency and quality in data handling.

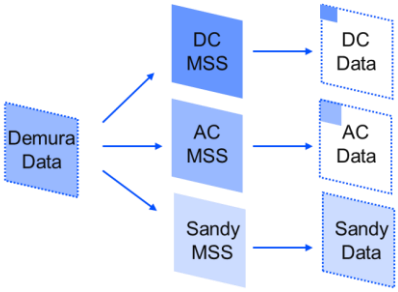

Figure 3. Multi-Scale Separation of Demura data.

As shown in Figure 4, this study also conducted multi-scale separation on Demura data under different DBV (Display Brightness Value) brightness conditions. Through analysis, it was found that DC data and AC data store the main characteristic information for Mura compensation, and this information varies with different DBV brightness levels. AC data exhibits significant similarity across different DBV brightness levels. In contrast, Sandy data under different DBV brightness levels does not possess distinct characteristic features and is more akin to random data. As illustrated in Figure 5, Sandy data at different positions on the AMOLED display panel under various DBV brightness levels also demonstrates the same characteristics, further validating this conclusion.

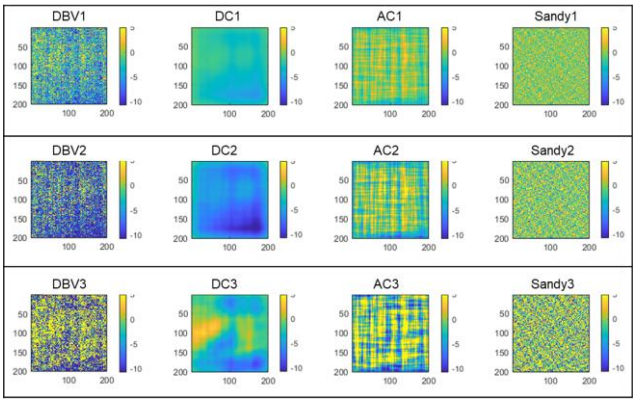

Figure 4. Data Analysis of Demura data.

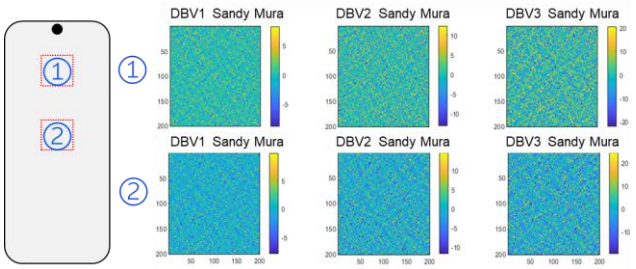

Figure 5. Data Analysis of Demura data.

Under different brightness conditions, the Mura compensation data of AMOLED display panels exhibit notable differences. Among them, the compensation data of DC data and AC data contain distinct features, allowing for the use of larger blocks for compression processing. This approach not only results in a smaller data volume but also simplifies the processing. However, Sandy Mura presents pixel-level fine textures, and the volume of its compensation data grows exponentially with an increase in resolution. This undoubtedly poses a core challenge in the data compression process, presenting a significant obstacle to efficient data handling.

2.4 Segmentation-Guided Image Compression

As shown in Figure 6, based on the spatial structural similarity of Sandy data under different dynamic brightness variation (DBV) conditions (quantitatively evaluated using the Structural Similarity Index, SSIM), this study employed a multiple image segmentation strategy to jointly process three sets of Sandy data—DBV1, DBV2, and DBV3—extracting spatial structural features and regional information under each brightness condition. Furthermore, for each structural layer of the segmented images, a cross-DBV condition (DBV1-DBV2-DBV3) structural similarity assessment was conducted. By applying the Non-Maximum Suppression (NMS) algorithm, co-occurring structures across the three datasets were merged and retained, achieving structural consistency integration across multiple brightness conditions. Finally, based on the Multi-Intensity Strength Characterization Model (MIS Intensity), differential modeling of the intensity distribution characteristics of DBV1, DBV2, and DBV3 was performed, completing the

compression processing of the shared similarity structures in Sandy data.

Using the same approach, this study also applied compression processing of shared similarity structures to AC data after block compression, further enhancing the compression ratio.

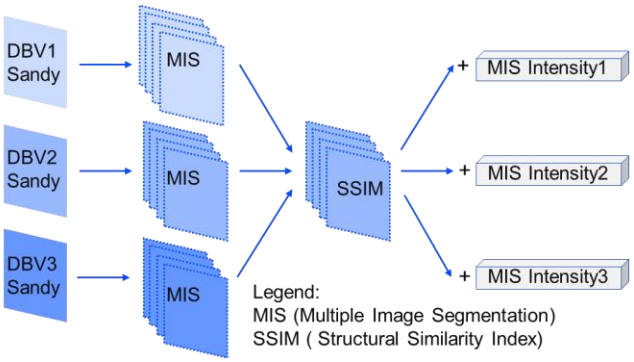

Figure 6. Hierarchical Segmentation and Adaptive Reconstruction for Lossy Compression.

3. Methods Verification and test results

Based on the tests carried out 6.6-inch AMOLED display module with a resolution of 1264×2800, we simultaneously compressed the 8-bit compensation data for five images with different brightness levels. The original data volume was 68 Mbit, and after compression, it was reduced to approximately 7.5 Mbit, achieving a compression rate of 88.9%. As shown in Table 1, we assessed the Peak Signal-to-Noise Ratio (PSNR) [6]and Structural Similarity Index (SSIM) between the decompressed data and the original data. Under the three different Display Brightness Values (DBVs), the average PSNR was approximately 41.4 dB, and the average SSIM was approximately 0.950, demonstrating outstanding compression performance. The decompression circuit is also not overly complex, with an RTL Gatecount of approximately 50~80K.

Table 1. Compression Performance of Compensation data at Different Brightness Levels.

Brightness	PSNR(dB)	SSIM	Evaluation
DBV1	54.4	0.998	Excellent
DBV2	38.1	0.955	Excellent
DBV3	31.8	0.901	Good

As illustrated in Figure 7 the compensation effect at the three different DBV brightness levels can achieve a nearly lossless compression result as expected.

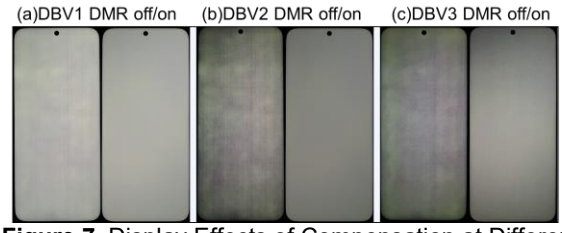

Figure 7. Display Effects of Compensation at Different Brightness Levels.

4. Conclusion

In summary, this study addresses the issue of low storage efficiency in Demura compensation data for AMOLED displays by integrating a high-performance compression scheme that combines multi-dimensional feature extraction optimization with adaptive encoding strategies. The proposed approach achieves significant storage reduction (with a compression ratio of 88.9%) by segregating Mura data into three distinct components—DC, AC, and Sandy—and compressing each independently. While minimizing storage requirements, it maintains exceptional image quality, as evidenced by an average Peak Signal-to-Noise Ratio (PSNR) of 41.4 dB and a Structural Similarity Index (SSIM) of 0.950. Furthermore, the decompression circuit exhibits low complexity (50–80K gates), making it well-suited for high-end display devices and high-resolution applications, ultimately delivering near-lossless compression performance.

5. Reference

1. Lee J, Kim S. Demura compensation algorithm for high-resolution AMOLED displays using machine learning. IEEE Trans Electron Devices. 2021;68(5):2345-2352.
2. Park S, Choi D, Jung Y. Low-complexity compression algorithm for real-time Demura in 8K AMOLED displays. SID Symp Dig Tech Pap. 2023;54:1023-1026.
3. Lee J, Kim S. Demura compensation algorithm for high-resolution AMOLED displays using machine learning. IEEE Trans Electron Devices. 2021;68(5):2345-2352.
4. Wang Q, Wu T, Li M. Data compression techniques for Demura compensation in AMOLED: A review. Opt Express. 2022;30(10):16500-16515.
5. Wang Z, Bovik AC, Sheikh HR, Simoncelli EP. Image quality assessment: From error visibility to structural similarity. IEEE Trans Image Process. 2004;13(4):600-612.
6. Horé A, Ziou D. Image quality metrics: PSNR vs. SSIM. IEEE Computer Society. 2010. DOI:10.1109/ICPR.2010.579.